

Downregulation of Mcl-1 through inhibition of translation contributes to benzyl isothiocyanate-induced cell cycle arrest and apoptosis in human leukemia cells

T Zhou^{1,5}, G Li^{1,5}, B Cao^{1,5}, L Liu¹, Q Cheng², H Kong¹, C Shan³, X Huang¹, J Chen⁴ and N Gao^{*1}

Benzyl isothiocyanate (BITC) is one of the compounds of ITCs' family that has attracted a great deal of interest because of its ability to exhibit anticancer activity. In this study, we investigated the effects of BITC on cell cycle arrest and apoptosis in human leukemia cell lines, primary leukemia cells, and nude mice Jurkat xenograft. Exposure of Jurkat cells to BITC resulted in dose- and time-dependent increase in apoptosis, caspase activation, cytochrome *c* release, nuclear apoptosis-inducing factor (AIF) accumulation, Bcl2-associated X protein (Bax) translocation, and myeloid cell leukemia-1 (Mcl-1) downregulation. Treatment with these cells also resulted in cell cycle arrest at the G2/M phase. The G2/M-arrested cells are more sensitive to undergoing Mcl-1 downregulation and apoptosis mediated by BITC. BITC downregulates Mcl-1 expression through inhibition of translation, rather than through a transcriptional, post-translational, or caspase-dependent mechanism. Dephosphorylation of eukaryotic initiation factor 4G could contribute to the inhibition of Mcl-1 translation mediated by BITC. Furthermore, ectopic expression of Mcl-1 substantially attenuates BITC-mediated lethality in these cells, whereas knockdown of Mcl-1 through small interfering RNA significantly enhances BITC-mediated lethality. Finally, administration of BITC markedly inhibited tumor growth and induced apoptosis in Jurkat xenograft model in association with the downregulation of Mcl-1. Taken together, these findings represent a novel mechanism by which agents targeting Mcl-1 potentiate BITC lethality in transformed and primary human leukemia cells and inhibitory activity of tumor growth of Jurkat xenograft model.

Cell Death and Disease (2013) 4, e515; doi:10.1038/cddis.2013.41; published online 28 February 2013

Subject Category: Cancer

Anticarcinogenic effect of cruciferous vegetables is attributed to organic isothiocyanates (ITCs) that occur naturally as thioglucoside conjugates.¹ Benzyl isothiocyanate (BITC) is one of the compounds of ITCs' family that has attracted a great deal of interest because of its ability to inhibit chemically induced cancer in animal models.^{1,2} For instance, BITC is a potent inhibitor of mouse lung carcinogenesis and rat hepatocarcinogenesis mediated by tobacco-smoke and diethylnitrosamine.^{3,4} Inhibition of benzo(a)pyrene-induced lung tumorigenesis and mammary carcinogenesis in MMTV-*neu* mice by BITC has also been documented.^{5,6} Preclinical data has illustrated that BITC emerges as a promising anticancer agent and it would be meaningful and challenging to develop this compound to be a novel antitumor drug.⁷ Currently, ITCs are in human clinical trial for treating cancer.⁸

Evidence supports that BITC exerts its antiproliferative effects through inducing cell cycle arrest and apoptosis.⁹ Several signaling pathways have been reported to be involved in BITC-triggered apoptosis, for example, p53-independent X-linked inhibitor of apoptosis (XIAP) downregulation, and reactive oxygen species (ROS) and Bcl2-associated X protein (Bax)/Bak-dependent pathway found in breast cancer cells,^{10,11} and ROS, p38- mitogen-activated protein kinases, signal transducer and activator of transcription-3, PI3K/Akt/Foxo, and nuclear factor- κ B signaling pathways found in pancreatic cancer cells.^{12–15} However, little is known about other signaling pathways involved in the regulation of BITC-induced apoptosis.

Several studies have been documented that myeloid cell leukemia-1 (Mcl-1) has a critical role in cell survival, particularly in malignant hematopoietic cells.¹⁶ Mcl-1

¹Department of Pharmacognosy, School of Pharmacy, 3rd Military Medical University, Chongqing, China; ²16th Team of Cadet Brigade, 3rd Military Medical University, Chongqing, China; ³15th Team of Cadet Brigade, 3rd Military Medical University, Chongqing, China and ⁴Department of Hematology, Southwest Hospital, 3rd Military Medical University, Chongqing, China

*Corresponding author: N Gao, Department of Pharmacognosy, School of Pharmacy, 3rd Military Medical University, 30 Gao Tan Yan Sha Ping Ba, Chongqing 400038, China. Tel: +86 23 68753736; Fax: +86 23 68753046; E-mail: gaoning59@yahoo.com.cn

⁵These authors contributed equally to this work.

Keywords: benzyl isothiocyanate; apoptosis; Mcl-1; translation; leukemia

Abbreviations: BITC, benzyl isothiocyanate; ITCs, isothiocyanates; ROS, reactive oxygen species; AML, acute myeloid leukemia; Mcl-1, myeloid cell leukemia-1; Bcl-2, B-cell lymphoma 2; XIAP, X-linked inhibitor of apoptosis; Bcl-xL, B-cell lymphoma-extra large; Bax, Bcl2-associated X protein; Bad, Bcl2-associated death promoter; PARP, poly-ADP-ribose polymerase; AIF, apoptosis-inducing factor; COX, cytochrome *c* oxidase; UV, ultraviolet; eIF, eukaryotic initiation factor; siRNA, small interfering RNA; TUNEL, TdT-mediated dUTP-biotin nick-end labeling; FBS, fetal bovine serum; CHX, cycloheximide; PI, propidium iodide

Received 31.10.12; revised 23.1.13; accepted 23.1.13; Edited by A Stephanou

overexpression has been shown in a variety of human leukemic cells,¹⁷ and also appears to be a key factor in the resistance of leukemia to conventional cancer therapy.¹⁸ Selective overexpression of Mcl-1 in hematopoietic tissues of transgenic mice promotes the survival of hematopoietic cells and enhances the outgrowth of myeloid cell lines.¹⁹ Mcl-1 downregulation is often sufficient to promote apoptosis in leukemic cells, suggesting that Mcl-1 can be a potential therapeutic target in the treatment of several human leukemias.^{18,20–22}

In this study, we report for the first time that BITC potentially induces G2/M cell cycle arrest and apoptosis in human leukemia cells in association with the downregulation of Mcl-1. These results indicate that BITC downregulates Mcl-1 expression through inhibition of translation, rather than through a transcriptional, post-translational, or caspase-dependent mechanism. Furthermore, ectopic expression of Mcl-1 substantially attenuates BITC-mediated lethality in these cells, whereas knockdown of Mcl-1 through small interfering RNA (siRNA) significantly enhances BITC-mediated lethality. Our *in vivo* results indicate that BITC-mediated inhibition of growth of mouse Jurkat xenograft tumors was in association with the downregulation of Mcl-1 and induction of apoptosis. The results of this study further elucidate the mechanism of BITC as an antileukemic agent.

Results

BITC potently induces apoptosis in dose- and time-dependent manners. A dose-dependent study in Jurkat cells revealed a moderate increase in apoptosis 12 h after exposure to 4 μ M BITC and very extensive apoptosis at concentrations of 6–8 μ M (Figure 1a). Time-course analysis of cells exposed to 8 μ M BITC demonstrated a significant increase in apoptosis as early as 3 h. These events became apparent after 6 h of drug exposure, and reached near-maximal levels after 12 h (Figure 1b).

Consistent with these findings, the same BITC concentrations and exposure intervals resulted in cleavage/activation of caspase-9 and -3, and degradation of poly-ADP-ribose polymerase (PARP) (Figure 1c). These events were also accompanied by the release of cytochrome *c* and nuclear apoptosis-inducing factor (AIF) accumulation (Figure 1c). The increased level of AIF was determined in the nucleus of cells treated with BITC in a time-dependent manner (Figure 1d).

Exposure of Jurkat cells to BITC results in the downregulation of Mcl-1 and translocation of Bax. The effects of BITC on the expression of antiapoptotic B-cell lymphoma 2 (Bcl-2) family proteins were examined in Jurkat cells. A marked dose-dependent decrease of Mcl-1 expression was noted in BITC-treated cells. Exposure of cells to 8 μ M BITC for 3 h resulted in a modest decrease in levels of Mcl-1. These events became apparent after 4 h and reached maximal effect after 6 h of drug exposure (Figure 1e). Furthermore, translocation of Bax from the cytosol to mitochondria was noted in cells treated with BITC (Figure 1e). In contrast, exposure of cells to BITC did not discernibly modify the expression of Bcl-2 family proteins, including Bcl-2, B-cell

lymphoma-extra large (Bcl-xL), XIAP, or Bcl-2-associated death promoter (Bad) (Figure 1f).

G2/M-arrested cells were susceptible to BITC-mediated downregulation of Mcl-1 and apoptosis. Exposure of cells to 2 μ M BITC resulted in a modest increase in percentages of cells at the G2/M phase. These events became more apparent after exposure of cells to 4 μ M BITC (Figure 2a). However, the population of cells at sub-G1 was observed in place of the G2/M population after exposure of cells to 8 μ M BITC. Therefore, BITC induces cell cycle arrest at the G2/M phase, and culminating in apoptosis in human leukemia cells.

To explore the mechanism by which BITC induces cell cycle arrest at the G2/M phase, we determined if BITC modulates the expression of G2/M cell cycle regulatory molecules using western blotting. Exposure of cells to BITC resulted in a marked decrease in levels of phospho-Cdc2 in a dose-dependent manner (Figure 2b). In contrast, BITC had little or no effect on the expression of cyclin A, cyclin B1, and Cdc2. These results suggest the possible involvement of Cdc2 dephosphorylation in BITC-mediated G2/M cell cycle arrest.

To determine whether G2/M-arrested cells are susceptible to the BITC-induced apoptosis, we examined the effect of BITC in cells synchronized at the G2/M phase by nocodazole treatment. Treatment of G2/M-synchronized cells with 4 μ M BITC resulted in a pronounced increase in the proportion of sub-G1 cell population and apoptosis (Figures 2c and d). Consistent with these findings, treatment of G2/M-synchronized cells with 4 μ M BITC also resulted in a marked increase in cleavage/activation of caspase-9 and -3, degradation of PARP, release of cytochrome *c*, and a pronounced decrease in levels of Mcl-1 (Figure 2e). Such findings suggest that G2/M-arrested cells might be sensitive to undergoing downregulation of Mcl-1 and induction of apoptosis-mediated by BITC.

BITC-induced lethality in association with Mcl-1 downregulation in multiple leukemia cell lines and primary human leukemia cells. To determine whether BITC-mediated lethality observed in Jurkat cells also occur in other leukemia cell lines, parallel studies were carried out in U937 and HL-60 cells. Exposure of Jurkat and U937 cells to 8 μ M BITC for 12 h resulted in a pronounced increase in apoptosis (Figure 3a). Also, these cells exhibited comparable degrees of caspase-9 and -3 activation, PARP degradation, cytochrome *c* release, and Mcl-1 downregulation (Figures 3b and c). However, HL-60 cells are more refractory to apoptosis induction by BITC than those cells, and exhibited less degrees of caspase-9 and -3 activation, cytochrome *c* release, and Mcl-1 downregulation.

To determine whether BITC could also trigger apoptosis in primary human leukemia cells, parallel experiments were carried out in primary leukemia blasts from eight acute myeloid leukemia (AML) patients. Exposure of these AML blasts to 8 μ M BITC for 24 h resulted in a marked increase in apoptosis (Figure 3d). Consistent with these findings, treatment of leukemia blasts from two AML patients with BITC also resulted in cleavage/activation of caspase-9 and -3, degradation of PARP, release of cytochrome *c*, and downregulation of Mcl-1

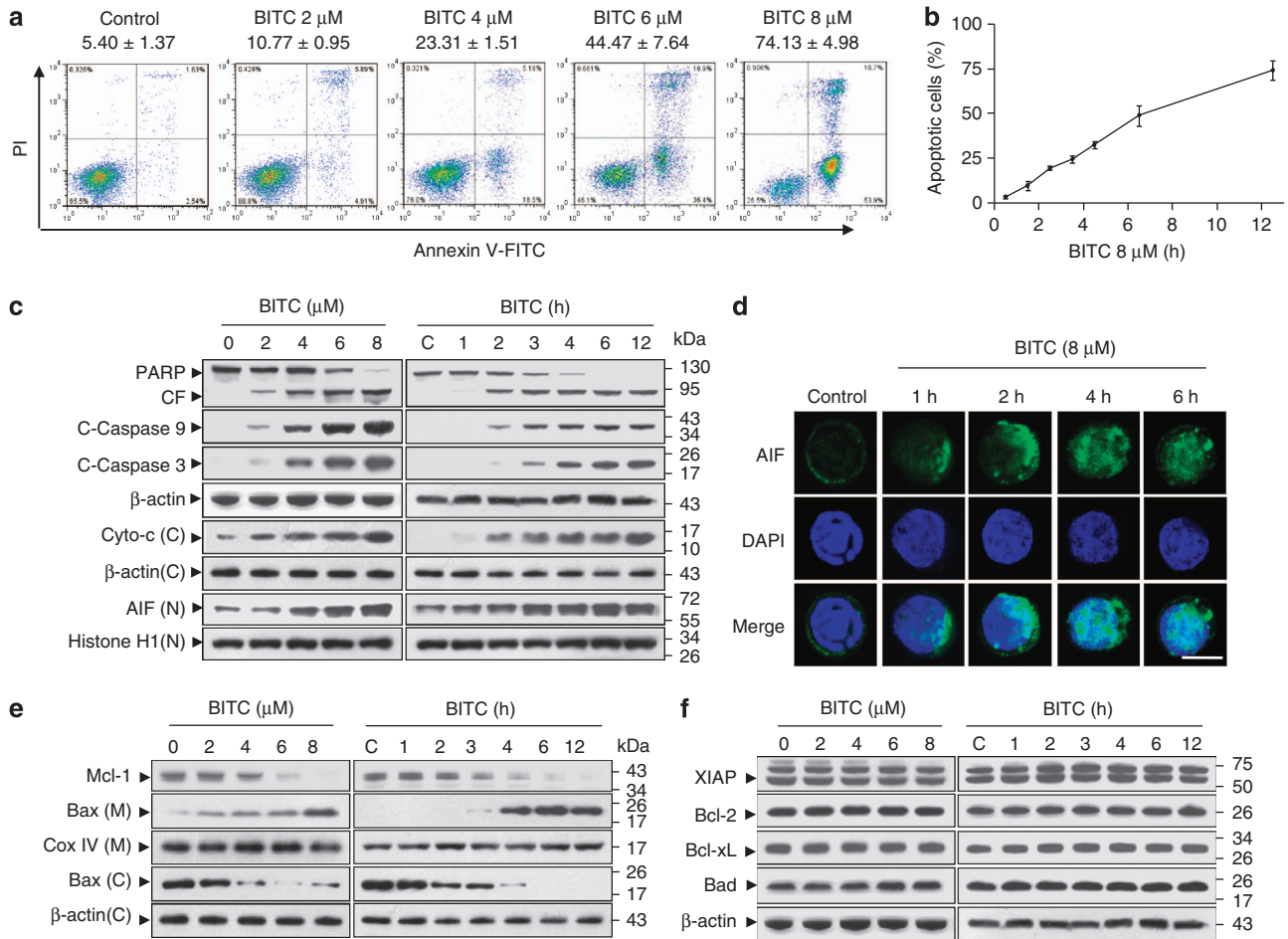


Figure 1 Treatment with BITC results in Mcl-1 downregulation, translocation of Bax, nuclear AIF accumulation, release of cytochrome c, caspase activation, and apoptosis in dose- and in time-dependent manners in Jurkat cells. (a) Jurkat cells were treated with 0, 2, 4, 6, and 8 μM BITC for 12 h. (b) The cells were treated with 8 μM BITC for 0, 1, 2, 3, 4, 6, and 12 h. In (a) and (b), cells were stained with Annexin V/PI, and the percentage of apoptotic cells was determined using flow cytometry. (c) After treatment with BITC, total cellular extracts, nuclear extracts, and cytosolic fractions were prepared and subjected to western blot analysis using antibodies against PARP, cleaved-caspase (C-Caspase)-9, cleaved-caspase-3, cytochrome c, and AIF. (d) AIF immunostaining (green) of Jurkat cells treated with 8 μM BITC for 0, 1, 2, 4, and 6 h, with 4',6-diamidino-2-phenylindole (DAPI) staining of the nucleus (blue). Scale bar represents 10 μm . (e and f) Western blot was used to analyze the expression of Mcl-1, Bax, XIAP, Bcl-2, Bcl-xL, and Bad. Blots were subsequently stripped and reprobed with antibody against β -actin, COX IV (mitochondrial fraction), and histone H1(nuclear extracts) to ensure equivalent loading. Each lane was loaded with 30 μg of protein. Two additional studies yielded equivalent results. C, cytosolic fractions; M, mitochondrial fractions; N, nuclear extracts

(Figure 3e). These findings indicate that BITC induces apoptosis in association with Mcl-1 downregulation in both human leukemia cell lines and primary leukemia blasts. In contrast, BITC exerted little toxicity toward normal human peripheral blood mononuclear cells (Figure 3f). No change in expression of Mcl-1 was noted in BITC-treated cells.

Downregulation of Mcl-1 by BITC proceeds through inhibition of translation. To elucidate the mechanism underlying Mcl-1 downregulation by BITC, Mcl-1 mRNA expression in BITC-treated cells was quantified using real-time RT-PCR. Notably, treatment of cells with 8 μM BITC for different time intervals did not alter the expression of Mcl-1 at mRNA levels (Figure 4a). Furthermore, treatment with BITC had no significant effect on luciferase driven by an Mcl-1 promoter (Figure 4b). Such findings suggest that BITC induces Mcl-1 downregulation through transcription-independent mechanism.

To determine whether the downregulation of Mcl-1 mediated by BITC occurs through post-translational mechanism, Jurkat cells were exposed to 8 μM BITC for various intervals in the presence or absence of the proteasome inhibitor MG132 (10 μM). Treatment with MG132 alone did not affect the decline of Mcl-1 levels. Exposure of cells to BITC resulted in the downregulation of Mcl-1 in a time-dependent manner (Figure 4c). However, pretreatment of cells with MG132 did not block the downregulation of Mcl-1 mediated by BITC. To validate the action of MG132, we used ubiquitin as a control protein, with levels clearly increased upon proteasomal inhibition (Figure 4d). These findings suggest that downregulation of Mcl-1 mediated by BITC does not occur through post-translational mechanism.

We also determined the effect of caspase inhibition on Mcl-1 stability. Although pretreatment with caspase inhibitor Z-VAD blocked BITC-induced apoptosis and caspase-9 and -3 activation, it blocked the downregulation of Mcl-1

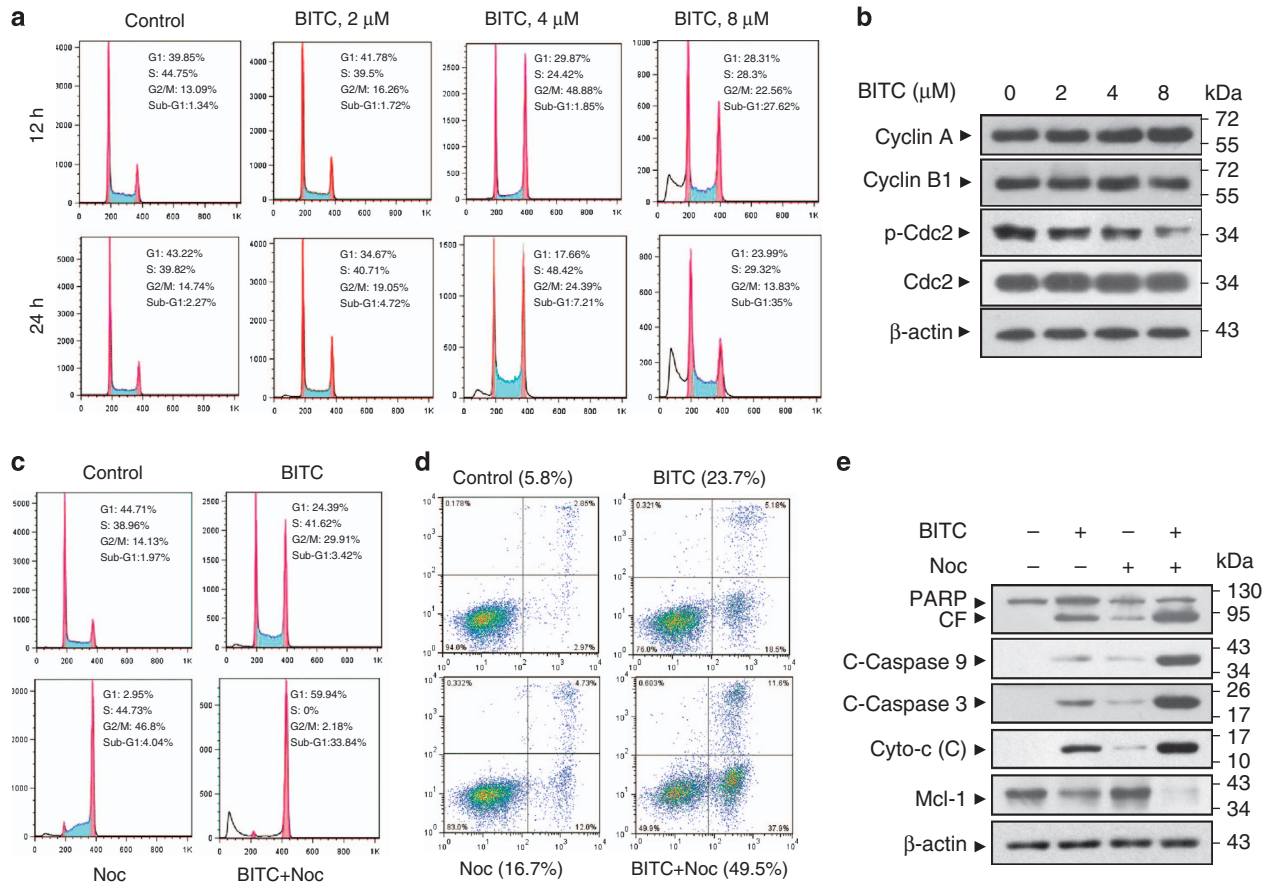


Figure 2 Effect of BITC on the cell cycle progression in Jurkat cells. **(a)** Jurkat cells treated with BITC at indicated concentrations for 12 and 24 h were stained with cell cycle staining solution as described in Materials and Methods, and analyzed using a flow cytometer. Cell cycle distribution (%) was measured using the FlowJo. **(b)** Jurkat cells treated with BITC at indicated concentrations for 12 h, whole-cell lysates were obtained and subjected to western blot analysis using antibodies against cyclin A, cyclin B1, Cdc2, phospho-Cdc2 (p-Cdc2), and β -actin. **(c)** Jurkat cells were pretreated with 100 ng/ml nocodazole for 12 h, followed by treatment with or without 4 μ M BITC for 12 h. After treatment, cells were stained with cell cycle staining solution as described in Materials and Methods, and analyzed using a flow cytometer. Cell cycle distribution (%) was measured using the FlowJo. **(d)** After the same treatment, cells were stained with Annexin V/PI, and the percentage of apoptotic cells was determined using flow cytometry. **(e)** Alternatively, the whole-cell lysates and cytosolic fractions were obtained and subjected to western blot analysis using antibodies against PARP, cleaved-caspase (C-Caspase)-9, cleaved-caspase-3, Mcl-1, cytochrome c, and β -actin. Each lane was loaded with 30 μ g of protein. Two additional studies yielded equivalent results

partly (Figures 4e and f). These findings demonstrate that Mcl-1 downregulation induced by BITC is affected by caspase inhibition, albeit not completely.

Lastly, we investigated the effect of protein synthesis inhibitor cycloheximide (CHX) on the downregulation of Mcl-1 mediated by BITC. Treatment with CHX alone reduced Mcl-1 protein level, and combined treatment with CHX and BITC decreased Mcl-1 protein level at an enhanced rate. Moreover, CHX prevented the accumulation ubiquitin proteins (Figure 5a). Such findings demonstrate that BITC-induced Mcl-1 downregulation could be caused by the inhibition of protein synthesis. To further confirm these possibilities, we pulse-labeled cells with [35 S]methionine and chased with or without BITC treatment. Newly synthesized Mcl-1 was analyzed by immunoprecipitation. Mcl-1 protein in cells prelabeled with [35 S]methionine was decreased at a similar rate following treatment without or with BITC, even though the total amount of Mcl-1 protein was dramatically decreased after BITC treatment, whereas no major changes were observed in protein synthesis of the housekeeping genes

hsp90 and β -actin (Figure 5b). These findings indicate that BITC induces Mcl-1 downregulation through inhibition of translation.

To identify changes in the translational efficiency of individual mRNAs during BITC-induced apoptosis, we isolated ribosomal fractions from extracts of cells treated with or without BITC. By ultracentrifugation in sucrose gradients, we separated the 40S and 60S complexes, which correspond to untranslated mRNAs (U in Figure 5c) and the polysomal fractions that contains mRNAs that are being efficiently translated into proteins (P in Figure 5c). Exposure of cells to BITC resulted in a considerable decrease in the amount of polysomes and a corresponding increase in the abundance of the 40S and 60S complexes (Figure 5c), suggesting that inhibition of protein translation occurs during BITC-induced apoptosis. We then quantified by real-time RT-PCR, the transcripts corresponding to actin and Mcl-1 mRNAs in both U and P fractions and plotted the P/U ratio (Figure 5d). Actin mRNA is actively translated in untreated cells, as indicated by a P/U ratio 2, whereas a ratio of 1.5 was observed for

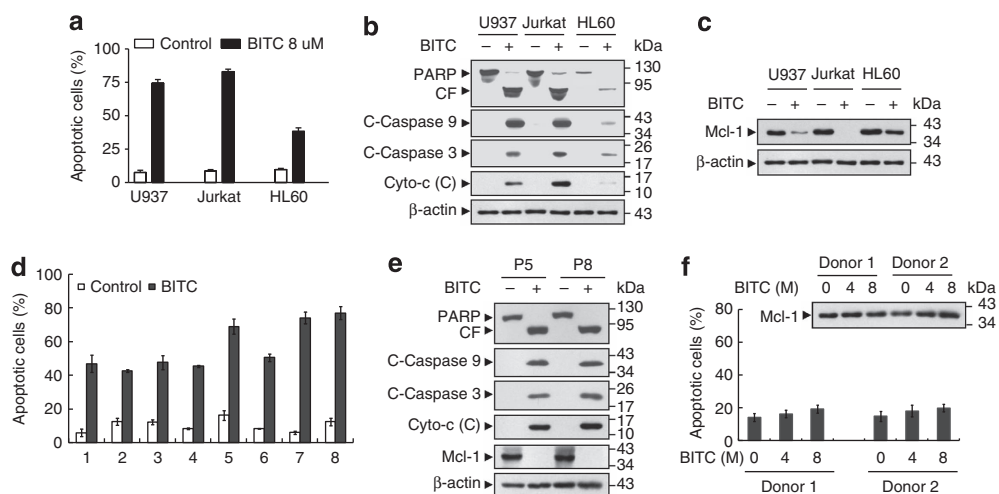


Figure 3 Exposure to BITC results in a marked increase in apoptosis in association with Mcl-1 downregulation in multiple leukemia cell lines and primary human leukemia cells but not normal human peripheral blood mononuclear cells. (a) U937, Jurkat, and HL-60 cells were treated with or without 8 μ M BITC for 12 h. After treatment, cells were stained with Annexin V/PI, and apoptosis was determined using flow cytometry as described in the Materials and Methods section. The values obtained from Annexin V/PI assays represent the mean \pm S.D. for three separate experiments. (b and c) Whole-cell lysates and cytosolic fractions (C) were obtained and subjected to western blot analysis using antibodies against PARP, cleaved-caspase (C-Caspase)-9, cleaved-caspase-3, cytochrome c, Mcl-1, and β -actin. (d) Primary leukemia blasts were isolated from the peripheral blood of eight patients with AML as described in the Materials and Methods section. After exposure to 8 μ M BITC for 24 h, the extent of apoptosis was determined using flow cytometry. The values obtained from Annexin V/PI assays represent the mean \pm S.D. for three separate experiments. (e) Whole-cell lysates and cytosolic fractions (C) in blasts from two AML patients were obtained and subjected to western blot analysis using antibodies against PARP, cleaved-caspase-9, cleaved-caspase-3, Mcl-1, cytochrome c, and β -actin. (f) Normal human peripheral blood mononuclear cells, exposed to designated concentration of BITC for 24 h, after which the extent of apoptosis was determined using flow cytometry. Alternatively, whole-cell lysates were obtained and subjected to western blot analysis to monitor expression of Mcl-1. Each lane was loaded with 30 μ g of protein. Two additional studies yielded equivalent results

Mcl-1 mRNA. This implies that the two mRNAs are being translated, although Mcl-1 mRNAs are present in lower amounts than actin. After BITC treatment, we observed a sharp decrease of polysome-associated Mcl-1 mRNAs ($P/U < 1$) and a slight decrease in the levels of the cap-dependent actin mRNAs. Our results indicate that cap-dependent translation might be preferentially impaired.

To elucidate further mechanism by which BITC might inhibit Mcl-1 translation, we examined the status of the initiation complex eukaryotic initiation factor (eIF)4E and eIF4G. Treatment with BITC for 2 h resulted in a striking suppression of eIF4G phosphorylation. These events became apparent after 3 h of drug exposure. Treatment with BITC also caused a decrease in the expression of total eIF4G at late time intervals (Figure 5e). However, treating with BITC resulted in a modest increase in levels of phospho-eIF4E after 2 h of drug exposure, and then returned to the initial level after 12 h of treatment. Furthermore, phosphorylation of the eIF4E-binding protein 1 declined after BITC treatment. These observations suggest that BITC-mediated inhibition of eIF4G phosphorylation may be involved in the inhibition of Mcl-1 translation.

Enforced expression of Mcl-1 substantially attenuates BITC-mediated apoptosis. To determine whether downregulation of Mcl-1 has a functional role in BITC-induced apoptosis, Jurkat cells stably overexpressing Mcl-1 were employed. Two selected populations of cells, Mcl-1(C8) and Mcl-1(C12), displayed two- to threefold increases in Mcl-1 protein levels compared with empty vector control cells (Figure 6a). Significantly, enforced expression of Mcl-1 attenuated BITC-mediated apoptosis, activation of

caspase-9 and -3, degradation of PARP, and release of cytochrome c (Figures 6a and b). Although a slight reduction in the expression of ectopic Mcl-1 was observed in infectants exposed to 8 μ M BITC, as one would expect of an inhibitor of translation, the Mcl-1 levels in BITC-treated infectant cells were higher than that in untreated control cells (Figure 6c). These data indicate that downregulation of Mcl-1 has a critical role in BITC-induced apoptosis in leukemia cells.

Knockdown of Mcl-1 by RNA interference enhances BITC-mediated apoptosis. To further confirm the functional role of Mcl-1 in BITC-mediated lethality in leukemia cells, Jurkat cells stably expressing Mcl-1 siRNA were employed. The knockdown of Mcl-1 in Jurkat cells led to a nearly two- to threefold increase in BITC-mediated apoptosis compared with control cells (Figure 6d). BITC was also considerably more effective in triggering the activation of caspase-9 and -3, degradation of PARP, and release of cytochrome c (Figure 6e). Furthermore, infection of cells with Mcl-1 siRNA reduced levels of total Mcl-1 compared with control cells. Exposure of these cells to BITC resulted in a significant reduction of Mcl-1 expression compared with control cells (Figure 6f). Taken together, these findings indicate that Mcl-1 downregulation has a significant functional role in BITC-mediated lethality.

BITC exhibits antitumor activity in xenografts of leukemia Jurkat cells by induction of apoptosis and downregulation of Mcl-1. The *in vivo* antitumor activity of BITC on leukemia Jurkat cells was further evaluated in a nude mouse xenograft model. Treatment with BITC resulted

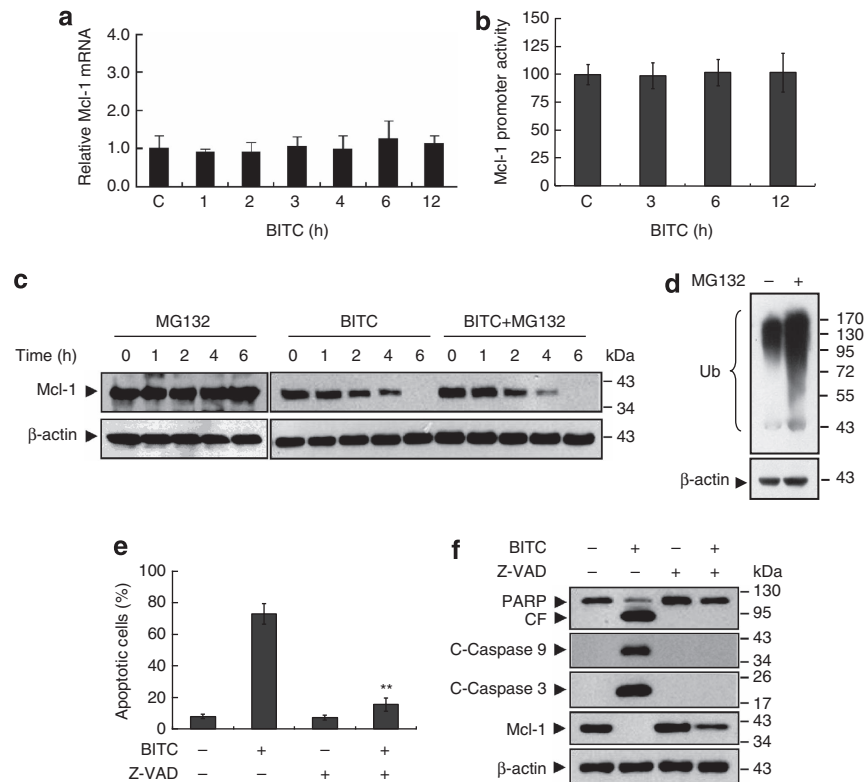


Figure 4 BITC induces Mcl-1 downregulation through the independent transcriptional and post-translational mechanisms. **(a)** Jurkat cells were treated with 8 μ M BITC at the designated intervals, after which total RNA were isolated and Mcl-1 mRNA were quantified using real-time reverse transcription-polymerase chain reaction (RT-PCR) as described in the Materials and Methods section. **(b)** Jurkat cells were cotransfected with (–203/+10-Mcl-1-pGL2) or pGL2-Basic and pRL-TK-luc plasmids. Cells were incubated for 12 h and then treated with BITC for 0, 3, 6, and 12 h, after which activity of firefly and *Renilla* luciferase was monitored as described in the Materials and Methods section. Values for firefly luciferase activity were normalized to those obtained for *Renilla* luciferase activity, after which values obtained for (–203/+10-Mcl-1-pGL2)-transfected cells were divided by the corresponding values obtained for pGL2-Basic-transfected cells. The graph shown represents the mean \pm S.D. in four separate experiments. **(c)** Jurkat cells were treated with MG132 (10 μ M), BITC (8 μ M), or cotreated with MG132 and BITC for different exposure intervals as indicated. Total cellular extracts were prepared and subjected to western blot assay using antibodies against Mcl-1 and β -actin. **(d)** Jurkat cells were treated with or without MG132 (10 μ M) for 4 h, and whole-cell lysates were obtained and subjected to western blot analysis using antibodies against ubiquitin (Ub) and β -actin. **(e)** Jurkat cells were pretreated with Z-VAD (10 μ M) for 2 h, followed by treatment with 8 μ M BITC for 12 h. After treatment, apoptosis was determined using flow cytometry. The values obtained from Annexin V/PI assays represent the mean \pm S.D. for three separate experiments. **Values for cells treated with BITC and Z-VAD were significantly reduced compared with values obtained for BITC alone by Student's *t*-test; $P < 0.01$. **(f)** Whole-cell lysates were obtained and subjected to western blot analysis using antibodies against PARP, cleaved-caspase (C-Caspase)-9, cleaved-caspase-3, Mcl-1, and β -actin

in a dramatic suppression of tumor growth 10 days following drug exposure ($P < 0.05$ versus vehicle control). These events became more apparent 15 and 20 days after drug exposure ($P < 0.01$ between BITC treatment and vehicle control) (Figure 7a). In contrast, no significant change in body weight was noted comparing vehicle control and BITC regimen (Figure 7b), indicating that no severe toxicity was observed.

We further determined apoptosis in tumor tissue of leukemia xenograft using TdT-mediated dUTP-biotin nick-end labeling (TUNEL) assay. TUNEL-positive apoptotic cells of tumor sections significantly increased in BITC-treated Jurkat xenograft mice compared with the control group. Exposure of mice to BITC also caused a rapid increase in immunoreactivity for cleaved-caspase-3 in tumor sections, indicative of apoptosis. Furthermore, Mcl-1 expression in tumor sections of Jurkat xenograft mice decreased upon BITC treatment (Figure 7c). Such findings suggest that BITC-mediated antileukemic activity *in vivo* is associated with the downregulation of Mcl-1.

Discussion

The results of this study indicate that treatment with BITC results in G2/M cell cycle arrest and apoptosis in human leukemia cells. Notably, this study demonstrates for the first time that downregulation of Mcl-1 through inhibition of translation has an important role in BITC-mediated lethality.

Extensive evidence is accumulating that Mcl-1 expression has a critical role in the survival of transformed cells,²³ particularly those of hematopoietic origin.²¹ The development of anticancer agents that diminish Mcl-1 protein levels has been the focus of intense interest. Indeed, a number of studies have documented Mcl-1 downregulation during apoptosis by a variety of agents, including ultraviolet (UV),²⁴ kinase inhibitor BAY43-9006,²⁵ growth factor withdrawal,²⁶ among others. Evidence revealed that Mcl-1 protein levels are regulated through several different mechanisms, including those operating at the transcriptional, translational, and post-translational levels. These results reveal that BITC induces a

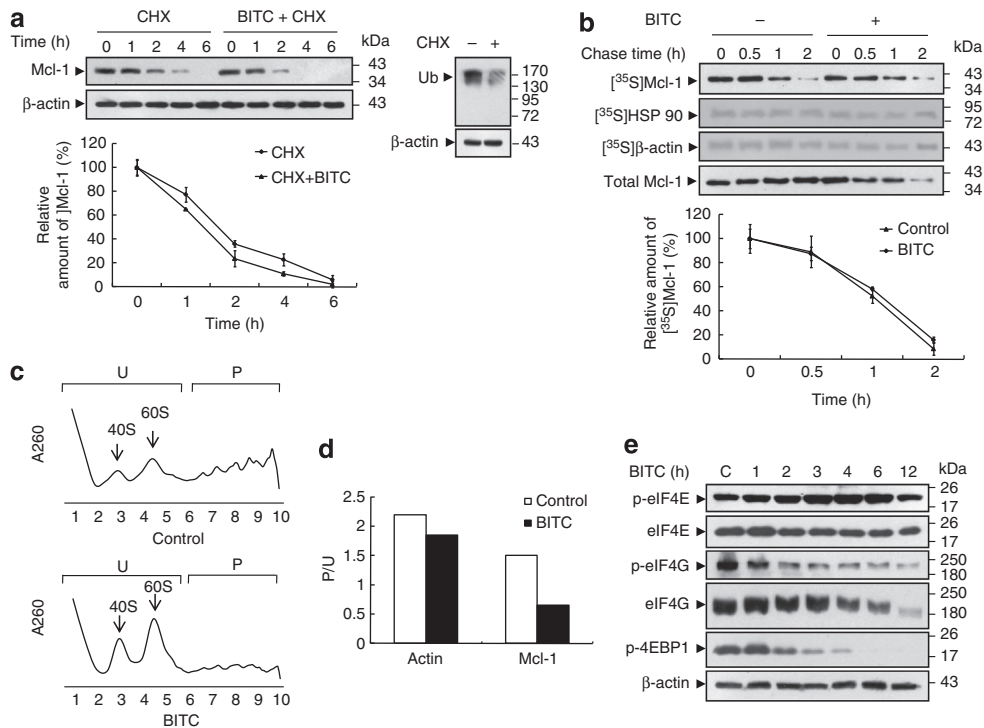


Figure 5 BITC induces Mcl-1 downregulation through inhibition of translation. (a) Jurkat cells were pretreated with 20 μ M CHX for 1 h, followed by treatment with or without 8 μ M BITC for varying intervals as indicated. After treatment, total cellular extracts were prepared and subjected to western blot assay using antibodies against Mcl-1 and β -actin. To validate the effect of CHX, Jurkat cells were treated with or without CHX (20 μ M) for 4 h. After treatment, whole-cell lysates were obtained and subjected to western blot analysis using antibodies against ubiquitin (Ub) and β -actin. (b) Jurkat cells were labeled with [³⁵S]methionine as described in the Materials and Methods section and chased for the designated periods in the presence or absence of BITC. At the end of the indicated intervals, synthesis of new Mcl-1, β -actin, and heat-shock protein 90 (hsp90) proteins were measured by immunoprecipitation. The immunoprecipitates were subjected to sodium dodecyl sulfate-polyacrylamide gel electrophoresis (SDS-PAGE), followed by autoradiography. In (a) and (b), densitometric analysis of the blots were performed by the Quantity One software and plotted with respect to time. (c) Lysates from cells treated without or with 8 μ M BITC for 6 h were fractionated by sucrose gradient centrifugation. The positions of the 40S and 60S ribosomal subunits are indicated. U, fraction containing untranslated/initiated mRNAs; P, polysomal fraction. (d) Amplification of actin and Mcl-1 mRNAs in U and P fractions by quantitative real-time reverse transcription-polymerase chain reaction (RT-PCR). The insets represent the P/U ratio in the control (white bars) or BITC-treated (black bars) cells for each mRNA tested. (e) Jurkat cells were treated with 8 μ M BITC for the designated periods. After treatment, total cellular extracts were prepared and subjected to western blot analysis using antibodies against phosphorylated (p)-eIF4E, eIF4E, p-eIF4G, eIF4G, p-4EBP1, and β -actin. Each lane was loaded with 30 μ g of protein. Two additional studies yielded equivalent results

rapid decrease in Mcl-1 protein levels. A critical question then arises regarding the mechanism by which Mcl-1 downregulation occurs during BITC treatment.

It has been shown that several cyclin-dependent kinase inhibitors, including flavopiridol, roscovitine, and SU9516, downregulate Mcl-1 expression in leukemia cells through inhibition of RNA polymerase II, leading to transcriptional repression.^{27–29} Our data indicated that BITC failed to decrease substantially Mcl-1 mRNA levels and promoter activity. These findings argue against the possibility that BITC downregulates Mcl-1 protein through inhibition of transcription.

Another major mechanism by which Mcl-1 protein level could be regulated is degradation by the proteasome system. It has been shown that the elimination of Mcl-1 via DNA damage can be blocked by MG132, a proteasome inhibitor, suggesting a role for the ubiquitin–proteasome pathway in apoptosis.³⁰ However, pretreatment with MG132 failed to block the downregulation of Mcl-1 mediated by BITC. Our findings argue strongly against the possibility that BITC downregulates Mcl-1 protein through the proteasome system. It should be noted that Mcl-1 can be the target of degradation

of caspase-3.³¹ Caspase-mediated cleavage might contribute to the downregulation of Mcl-1 expression as caspases can cleave Mcl-1 following two aspartic acid residues (Asp¹²⁷ and Asp¹⁵⁷). However, the findings that BITC-induced the downregulation of Mcl-1 was not completely attenuated by caspase inhibition, raising the possibility that factors other than caspase-mediated events are involved in this phenomenon.

Having ruled out the mechanism by which BITC induced downregulation of Mcl-1 through inhibition of transcription and the ubiquitin–proteasome pathway, the major remaining possibility is that BITC could downregulate Mcl-1 protein levels through inhibition of translation. Indeed, our results indicate that a marked inhibition of Mcl-1 translation was noted following exposure of cells to BITC. Notably, treatment with BITC slightly accelerated the clearance of Mcl-1 protein after inhibition of protein synthesis by CHX. However, BITC did not enhance the elimination of pre-existing Mcl-1 protein in cells prelabeled with [³⁵S]methionine, suggesting that inhibition of translation played a major role in BITC-induced downregulation of Mcl-1 protein levels. Generally, translation is primarily regulated by several initiation factors. The initiation complex eIF4F, a heterotrimeric protein composed of eIF4E, eIF4G,

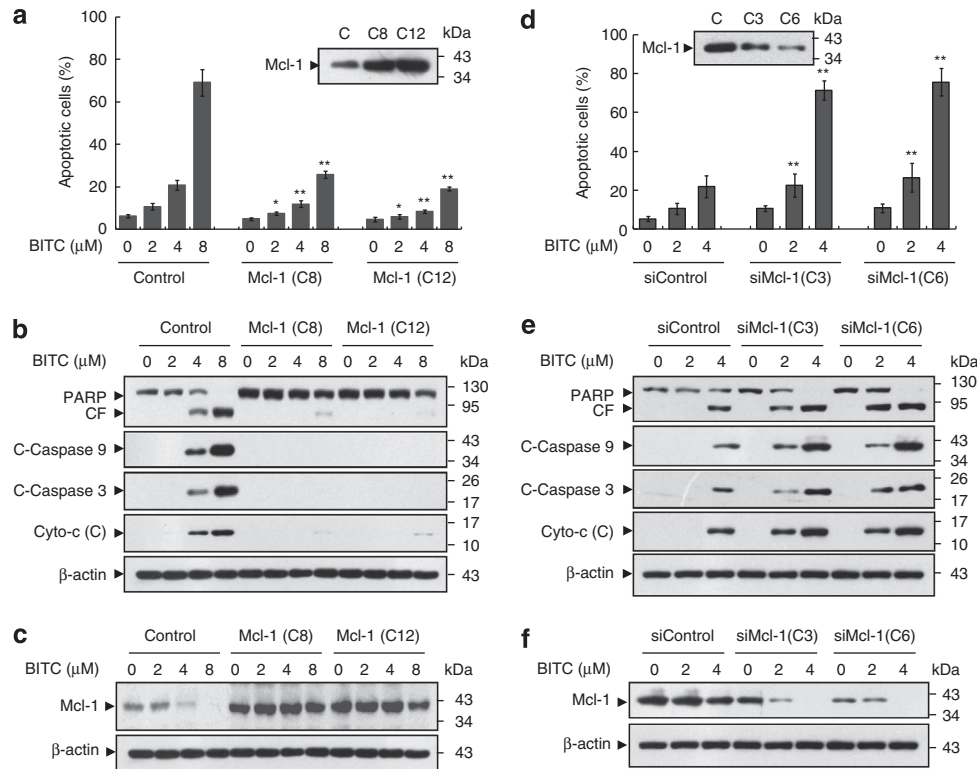


Figure 6 Enforced expression of Mcl-1 blocks BITC-mediated apoptosis, and diminished expression of Mcl-1 by siRNA enhances BITC-mediated apoptosis in Jurkat cells. (a) Total cellular extracts were prepared from an empty vector (Control) and two selected populations of cells (Mcl-1(C8) and Mcl-1(C12)) of Jurkat cells stably overexpressing Mcl-1, and then subjected to western blot assay using antibody against Mcl-1. Mcl-1(C8), Mcl-1(C12), and empty vector control cells were treated with 0, 2, 4, and 8 μM BITC for 12 h. After treatment, cells were stained with Annexin V/PI, and apoptosis was determined using flow cytometry as described in the Materials and Methods section. The values obtained from Annexin V/PI assays represent the mean ± S.D. for three separate experiments. **Values for Mcl-1(C8) and Mcl-1(C12) cells treated with BITC were significantly decreased compared with those for the empty vector control cells by the Student's *t* test; $P < 0.01$. (b and c) After treatment as indicated in (a), total cellular and cytosolic (C) fractions were prepared and subjected to western blot assay using antibodies against PARP, cleaved-caspase (C-Caspase)-9, cleaved-caspase-3, Mcl-1, cytochrome *c*, and β-actin. (d) Jurkat cells were stably infected with lentivirus containing siRNA specific for control (siControl) or Mcl-1 (siMcl-1), and total cellular extracts were prepared and subjected to western blot assay using antibody against Mcl-1. siMcl-1(C3), siMcl-1(C6), and siControl cells were treated with BITC at the indicated concentrations for 12 h. After treatment, cells were stained with Annexin V/PI, and apoptosis was determined using flow cytometry as described in the Materials and Methods section. The values obtained from Annexin V/PI assays represent the mean ± S.D. for three separate experiments. **Values for siMcl-1(C3) and siMcl-1(C6) cells treated with BITC were significantly increased compared with those for the siControl cells by the Student's *t* test; $P < 0.01$. (e and f) siMcl-1(C3), siMcl-1(C6), and siControl cells were treated with BITC at the indicated concentrations for 12 h, after which total cellular and cytosolic fractions were prepared and subjected to western blot assay using antibodies against PARP, cleaved-caspase-9, cleaved-caspase-3, Mcl-1, cytochrome *c*, and β-actin

and eIF4A, has a critical role in the translation of the mRNAs. The center of the eIF4F complex is eIF4G, a modular protein and the docking platform for several translation initiation factors and regulatory proteins, including mitogen-activated protein kinase-interacting kinases 1 and 2.³² The eIF4G family consists of three isoforms, including eIF4GI, eIF4GII, and p97/DAP5/NAT1. Both eIF4GI and eIF4GII are involved in cap-dependent translation, and p97/DAP5/NAT1 could be a caspase-activated translation factor that can mediate its own cap-independent translation.³³ The recent studies have indicated that phosphorylation of eIF4G at Ser1108 has been characterized as correlating with translation.³⁴ The anabolic agents, such as insulin, increase the phosphorylation of eIF4G at Ser1108 through a mammalian target of rapamycin-dependent pathway.³⁵ Insulin-like growth factor-1 induces regulation of cap-dependent translation through eIF4G phosphorylation, suggesting that eIF4G phosphorylation is a molecular marker associated with enhanced cap-dependent translation.³⁶ In this context, BITC potently suppressed

phosphorylation of eIF4G at Ser1108 at early time point of BITC exposure, suggesting that inhibition of eIF4G phosphorylation could be responsible for BITC-mediated downregulation of Mcl-1 through inhibition of cap-dependent translation. By using polysome analysis and quantitative real-time RT-PCR, our data also indicates that BITC downregulates Mcl-1 through inhibition of cap-dependent translation, further confirming that inhibition of cap-dependent translation through dephosphorylation of eIF4G could contribute to BITC-mediated Mcl-1 downregulation. A clearer characterization of the functional role of eIF4G dephosphorylation in the disruption of Mcl-1 translation by BITC awaits further study.

It is significant that enforced expression of Mcl-1 markedly diminished BITC-mediated lethality in Jurkat cells, arguing that downregulation of Mcl-1 has a critical role in BITC-related lethality. Consistent with this notion, Mcl-1 overexpression largely inhibited caspase activation and cytochrome *c* release. These findings are consistent with previous study, which demonstrated that Mcl-1 operates upstream of cytochrome *c*

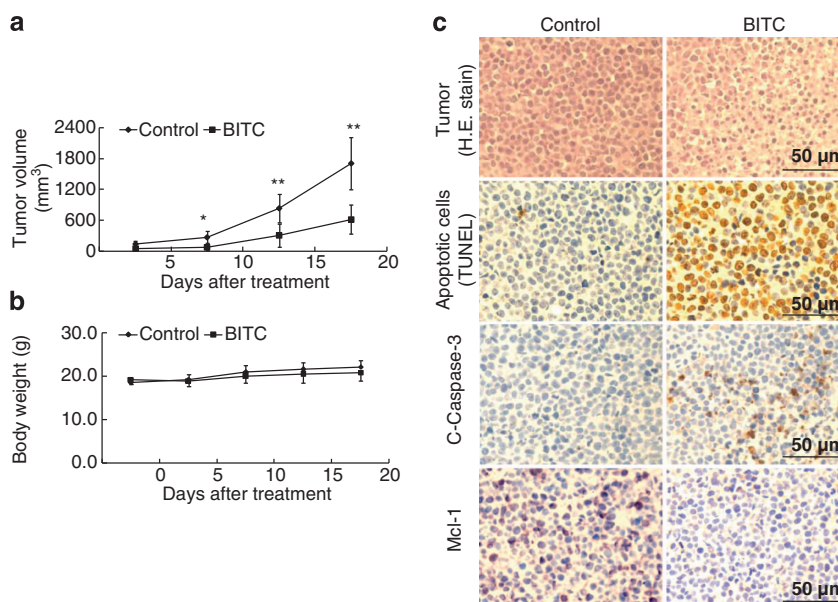


Figure 7 BITC exhibits antitumor activity and induces apoptosis in the xenograft animal model. (a) A 5-week-old nude mice inoculated subcutaneously with Jurkat cell ($2 \times 10^6/0.2$ ml per mouse). At 3 days after tumor inoculation, mice were randomized into a control group (10 mice per group) and a treated group (10 mice per group, BITC 50 mg/kg, intraperitoneally, daily). Tumor volume assessment were conducted as described in the Materials and Methods section. Data are means \pm S.D. **Values of tumor volume for BITC treatment groups were significantly decreased compared with those for the control group by Student's *t*-test; $P < 0.05$. (b) Body weight of mice during the 20 days of BITC treatment. (c) Tumors were obtained from animals 20 days after drug exposure. Tumors were fixed and stained with hematoxylin and eosin (H&E) stain to examine tumor cell morphology, using TUNEL assay to determine apoptosis, and using immunohistochemistry to determine the levels of cleaved-caspase-3 (C-Caspase-3) and Mcl-1. The sections were lightly counterstained with 4',6-diamidino-2-phenylindole (DAPI) and photographed with a Scan Scope. Scale bar represents 50 μ m

release and caspase activation in UV-treated HeLa cells.²⁴ In addition, the knockdown of Mcl-1 in Jurkat cells led to a significant increase in BITC-mediated cytochrome *c* release, caspase activation, and apoptosis. Such findings are accordant with the studies that indicated that downregulation of Mcl-1 through siRNA is sufficient to induce apoptosis in multiple myeloma cells.³⁷

Previous studies have shown that BITC markedly inhibits tumor growth of human breast and pancreatic cancer cell xenografts.^{7,14} However, little is known about inhibitory effects of BITC on tumor growth of human leukemia xenograft model. In our studies using a nude mice Jurkat xenograft model, tumor volumes were reduced compared with controls after BITC treatment, indicating an antileukemia activity of this compound. To further validate the apoptotic mechanism found *in vitro*, we next examined the TUNEL staining, cleaved-caspase-3, and Mcl-1 expression in tumor specimens obtained from control- and BITC-treated animals. The increase in TUNEL-positive cells, caspase-3 activation, and the decrease in Mcl-1 expression were detected in the BITC-treated xenografts compared with the control group. To the best of our knowledge, this is the first report that describes an effective extrapolation of the *in vitro* apoptosis-inducing effects of BITC on the leukemia cells to the *in vivo* situation.

In conclusion, these findings indicate that BITC effectively induces apoptosis in human leukemia cell lines, primary AML blasts, and leukemia xenograft. This effect occurs in association with the downregulation of Mcl-1 through inhibition of translation, leading, in turn, to Bax translocation and nuclear AIF accumulation, and culminating in cytochrome *c* release and caspase activation. Dephosphorylation of eIF4G could

contribute to the inhibition of Mcl-1 translation mediated by BITC. This study could provide a better understanding of how BITC exerts its antileukemic activity *in vivo* and aid in developing this compound to treat leukemia and possibly other hematologic malignancies.

Materials and Methods

Chemicals and reagents. BITC was purchased from LKT Laboratories (St. Paul, NM, USA). Z-VAD-FMK, MG132, and CHX were from EMD Biosciences (La Jolla, CA, USA), and nocadazole was from Sigma-Aldrich (St. Louis, MO, USA). Antibodies against AIF, cytochrome *c*, cyclin A, cyclin B1, cdc-2, histone H1, and β -actin were purchased from Santa Cruz Biotechnology (Santa Cruz, CA, USA); Bcl-xL, XIAP, cytochrome *c* oxidase (COX) IV, Bad, ubiquitin, eIF4E, phospho-eIF4E (Ser209), phospho-4E-BP1 (Thr37/46), eIF4G, phospho-eIF4G (Ser1108), phospho-cdc2 (Tyr15), cleaved-caspase-3, and cleaved-caspase-9 were purchased from Cell Signaling Technology (Beverly, MA, USA); Bcl-2, Mcl-1, and Bax were purchased from BD Pharmingen (San Diego, CA, USA); Mcl-1 for immunohistochemistry was purchased from Abcam (Cambridge, MA, USA); and PARP was purchased from Epitomics (Burlingame, CA, USA).

Cell culture. Jurkat, U937, and HL-60 cells were purchased from American Type Culture Collection (ATCC, Manassas, VA, USA) and cultured in RPMI 1640 medium containing 10% fetal bovine serum (FBS).

Normal human peripheral blood mononuclear cells were obtained from blood samples collected from healthy volunteers. Peripheral blood samples were obtained from eight patients with newly diagnosed AML after informed consent. Approval was obtained from the Southwest Hospital (Chongqing, China) institutional review board for these studies. AML blasts were isolated by density gradient centrifugation over Histopaque-1077 (Sigma Diagnostics, St. Louis, MO, USA) at $400 \times g$ for 38 min. Isolated mononuclear cells were washed and assayed for total number and viability using Trypan blue exclusion. Blasts were suspended at 8×10^5 /ml and incubated in RPMI 1640 medium containing 10% FBS in 24-well plates.

Human Mcl-1 lentiviral construct was generated by inserting human full-length Mcl-1 cDNA into Ubi-MCS-3FLAG-IRES-puromycin lentiviral vector (GeneChem, Shanghai, China). The human Mcl-1 lentiviral expression plasmid or

GFP-puromycin-LV vector was cotransfected into 293Ta cells with the Lenti-Pac HIV Packaging Mix (GeneChem, Shanghai, China). Lentivirus-containing supernatants were harvested 48 h after transfection. To establish stable Mcl-1-overexpressing cell lines, Jurkat cells were transduced with serial dilutions of lentiviral supernatant in the presence of 5 μ g/ml polybrene and selected by 5 μ g/ml puromycin. Thereafter, cells from each population of cells were analyzed for Mcl-1 expression by western blot. And two selected populations of cells, designated C8 and C12, which displayed overexpression of Mcl-1 compared with empty vector controls (Ubi-MCS-EGFP-3FLAG-2A-Puro), were used in all experiments.

Western blotting. The total cellular samples were washed two times with ice-cold PBS and lysed in 1 \times NuPAGE LDS sample buffer (Invitrogen, Carlsbad, CA, USA). The protein concentration was determined using Enhanced BCA Protein Assay Reagent (Beyotime, Jiangsu, China) and 30 μ g of sample proteins were separated by SDS-PAGE, and transferred to PVDF membrane. Membranes were blocked with 5% fat-free dry milk in Tris-buffered saline containing 0.05% Tween-20 and incubated with antibodies. Protein bands were detected by incubating with horseradish peroxidase-conjugated antibodies (Kirkegaard and Perry Laboratories, Gaithersburg, MD, USA) and visualized with enhanced chemiluminescence reagent (Perkin-Elmer Life Sciences, Boston, MA, USA).

Apoptosis assay. Apoptotic cells were measured by staining with FITC-conjugated Annexin V/propidium iodide (PI) (BD Pharmingen, San Diego, CA, USA) and determining with flow cytometer according to the manufacturer's instructions as described previously.³⁸ Both early apoptotic (Annexin V-positive, PI-negative) and late apoptotic (Annexin V-positive and PI-positive) cells were included in cell death determinations.

Cell cycle analysis. Cell cycle analysis was performed on the harvested cell pellets treated with 0.1% Triton X-100, 3.8 mM Na citrate in ddH₂O, and PI solution (50 μ g/ml) containing RNase B (7 kU/ml). The mixture was analyzed by a flow cytometer after 30 min. The cell cycle distribution was measured using the FlowJo software (Treestar, Ashland, OR, USA).

Mcl-1 pulse-chase. Jurkat cells were plated at a density of 5 \times 10⁶ cells, in methionine-free RPMI for 30 min, and then labeled with 100 μ Ci/ml [³⁵S]methionine (ICN; Biomedicals Inc., Irvine, CA, USA) for 60 min at 37 °C. Cells were then washed in PBS and cultured in complete RPMI containing fetal bovine serum and excess of cold methionine (10 mM) and cysteine (5 mM) for the indicated periods in the presence or absence of 8 μ M BITC. At the end of the indicated intervals, cells were collected and subsequently subjected to immunoprecipitation using Mcl-1 antibody as described above. The immunoprecipitates were subjected to SDS-PAGE followed by autoradiography.

RNA interference. Oligonucleotides with the following targeting sequences were used for the cloning of small hairpin RNA-encoding sequences in hU6-MCS-ubiquitin-EGFP-IRES-puromycin lentiviral RNAi vector: Mcl-1, 5'-GCTAACACTT GAAGACCATA-3'. After cotransfection of lentiviral packaging plasmids into 293Ta cells, lentivirus-containing supernatants were harvested 48 h after transfection. Jurkat cells were infected with the lentiviral supernatant plus 5 μ g/ml polybrene and selected by 5 μ g/ml puromycin. Thereafter, cells from each clone were analyzed for Mcl-1 expression by western blot. And two selected populations of cells, designated C3 and C6, were used in all experiments.

Confocal immunofluorescence microscopy. At the end of each incubation, cells were fixed with 4% paraformaldehyde at room temperature for 30 min, permeabilized by 0.1% Triton X-100 in PBS at room temperature for 15 min, and then blocked nonspecific binding with 3% bovine serum albumin in PBS for 30 min at room temperature. Cells were further incubated with primary polyclonal anti-AIF antibody at 4 °C overnight, followed by secondary antibody (Alexa Fluor 647 donkey anti-rabbit IgG; Invitrogen) for 1 h. After washing, the nuclei were counterstained with 0.1 μ g/ml DAPI (Sigma-Aldrich Co., St. Louis, MO, USA) for 10 min, and then sealed in antifade reagent (Beyotime, Jiangsu, China). Confocal micrographs were scanned by a laser confocal scanning microscope TCS SP5; Leica Microsystems, Mannheim, Germany.

Analysis of nuclear AIF, cytosolic cytochrome c, and Bax and mitochondrial Bax. For nuclear fractionations, cells (2 \times 10⁶) were fractionated by Nuclear and Cytoplasmic Protein Extraction Kit (Beyotime) according to the

manufacturer's instructions. Mitochondrial and cytosolic fractions were obtained as described previously.²⁷ These fractions were prepared and subjected to western blot assay to monitor expression of AIF, cytochrome c, and Bax.

Polysome analysis. Sucrose gradient centrifugation was used to separate ribosomes into polysomal and subpolysomal forms. After centrifugation, gradients were collected into 10 fractions, while UV absorbance was recorded at 260 nm. The fractions corresponding to subpolysomes and polysomes were pooled. The RNA in the pooled fractions was extracted and analyzed by quantitative real-time RT-PCR.

Quantitative real-time RT-PCR. Total RNA and pooled sucrose gradient fractionated RNA were extracted using the RNeasy mini kit (Qiagen, Valencia, CA, USA). Quantitative real-time PCR analysis was carried out on an iCycler (Bio-Rad Laboratories, München, Germany) using the RealMasterMix (SYBR Green) (Tiangen Biotech, Beijing, China) according to the manufacturer's instructions. mRNA levels were normalized to β -actin level. Primers used for amplification of Mcl-1 and β -actin were purchased from Invitrogen. Sequences were as follows: β -actin – 5'-GGACTTCGAGCAAGAGATGG-3' (forward), 5'-AGCACTGTGTTGG CGTACAG-3' (reverse); Mcl-1 – 5'-TAAGGACAAAACGGGACTGG-3' (forward), 5'-ACCAGCTCCTACTCCAGCAA-3' (reverse).

Reporter gene assay. Jurkat cells were cotransfected with a –203/+10-Mcl-1-pGL2 plasmid (kindly provided by Dr. PK Burnette, Moffitt Research Center, Tampa, FL, USA), in which firefly luciferase is driven by the –203 to +10 element of the Mcl-1 gene promoter, or the pGL2-basic empty vector (Promega, Madison, WI, USA) and pRL-TK-luc plasmid encoding for *Renilla* luciferase. Cells were incubated for 12 h and then treated with BITC for an additional 12 h, after which the activity of firefly and *Renilla* luciferases was measured using the Dual-Luciferase reporter assay system (Promega). Values for firefly luciferase activity were normalized to those obtained for *Renilla* luciferase activity.

Xenograft model and immunohistochemical evaluation. Nude mice (5 weeks old) were purchased from Vital River Laboratories (Beijing, China). Animal experiments were approved by the Institutional Animal Care and Use Committee (IACUC) of the university. Jurkat cells (2 \times 10⁶/0.2 ml per mouse) were suspended in sterile PBS and injected subcutaneously into the right flank of the mice. Mice were randomly assigned in two groups of 10 mice per group. At 3 days after tumor inoculation, the treatment group received BITC (50 mg/kg, intraperitoneally for 20 days). The control group received an equal volume of solvent control. Tumor size and body weight were measured every 5 days. Tumor volumes were determined by a caliper and calculated according to the formula (width² \times length)/2. All animals were killed immediately after 20 days of drug exposure.

TUNEL assay. Apoptosis in tumor tissue sections was determined using In Situ Cell Death Detection kit (Roche, Mannheim, Germany). Briefly, tumor tissue sections of formalin-fixed, paraffin-embedded specimens were dewaxed in xylene and rehydrated in a graded series of ethanol. The tumor samples were incubated with proteinase K (2 mg/ml), and the TUNEL staining was performed according to the manufacturer's instructions.

Statistical analysis. Densitometric analysis was performed using the Quantity One software (Bio-Rad) to determine the relative abundance of protein expression. The values were presented as means \pm S.D. for at least three independent experiments. Student's *t*-test were used for statistical analysis. *P* < 0.05 (*) or *P* < 0.01 (**) was considered significantly different.

Conflict of Interest

The authors declare no conflict of interest.

Acknowledgements. This work was supported by the National Natural Science Foundation of China, No. 30971288 (N.G.) and No. 30972468 (B.C.), Chongqing Natural Science Foundation, China, No. 2008BB5290 (B.C.).

1. Hecht SS. Inhibition of carcinogenesis by isothiocyanates. *Drug Metab Rev* 2000; **32**: 395–411.
2. Conaway CC, Yang YM, Chung FL. Isothiocyanates as cancer chemopreventive agents: their biological activities and metabolism in rodents and humans. *Curr Drug Metab* 2002; **3**: 233–255.

3. Witschi H, Uyeminami D, Moran D, Espiritu I. Chemoprevention of tobacco-smoke lung carcinogenesis in mice after cessation of smoke exposure. *Carcinogenesis* 2000; **21**: 977–982.
4. Sugie S, Okumura A, Tanaka T, Mori H. Inhibitory effects of benzyl isothiocyanate and benzyl thiocyanate on diethylnitrosamine-induced hepatocarcinogenesis in rats. *Jpn J Cancer Res* 1993; **84**: 865–870.
5. Yang YM, Conaway CC, Chiao JW, Wang CX, Amin S, Whysner J *et al*. Inhibition of benzo(a)pyrene-induced lung tumorigenesis in A/J mice by dietary *N*-acetylcysteine conjugates of benzyl and phenethyl isothiocyanates during the postinitiation phase is associated with activation of mitogen-activated protein kinases and p53 activity and induction of apoptosis. *Cancer Res* 2002; **62**: 2–7.
6. Warin R, Chambers WH, Potter DM, Singh SV. Prevention of mammary carcinogenesis in MMTV-neu mice by cruciferous vegetable constituent benzyl isothiocyanate. *Cancer Res* 2009; **15**: 9473–9480.
7. Warin R, Xiao D, Arlotti JA, Bommareddy A, Singh SV. Inhibition of human breast cancer xenograft growth by cruciferous vegetable constituent benzyl isothiocyanate. *Mol Carcinogen* 2010; **49**: 500–507.
8. Lamy E, Scholtes C, Herz C, Mersch-Sundermann V. Pharmacokinetics and pharmacodynamics of isothiocyanates. *Drug Metab Rev* 2011; **43**: 387–407.
9. Miyoshi N, Uchida K, Osawa T, Nakamura Y. A link between benzyl isothiocyanate-induced cell cycle arrest and apoptosis: involvement of mitogen-activated protein kinases in the Bcl-2 phosphorylation. *Cancer Res* 2004; **64**: 2134–2142.
10. Kim SH, Singh SV. P53-independent apoptosis by benzyl isothiocyanate in human breast cancer cells is mediated by suppression of XIAP expression. *Cancer Prev Res (Phila)* 2010; **3**: 718–726.
11. Xiao D, Vogel V, Singh SV. Benzyl isothiocyanate-induced apoptosis in human breast cancer cells is initiated by reactive oxygen species and regulated by Bax and Bak. *Mol Cancer Ther* 2006; **5**: 2931–2945.
12. Sahu RP, Zhang R, Batra S, Shi Y, Srivastava SK. Benzyl isothiocyanate-mediated generation of reactive oxygen species causes cell cycle arrest and induces apoptosis via activation of MAPK in human pancreatic cancer cells. *Carcinogenesis* 2009; **30**: 1744–1753.
13. Sahu RP, Srivastava SK. The role of STAT-3 in the induction of apoptosis in pancreatic cancer cells by benzyl isothiocyanate. *J Natl Cancer Inst* 2009; **101**: 176–193.
14. Boreddy SR, Pramanik KC, Srivastava SK. Pancreatic tumor suppression by benzyl isothiocyanate is associated with inhibition of PI3K/AKT/FOXO pathway. *Clin Cancer Res* 2011; **17**: 1784–1795.
15. Srivastava SK, Singh SV. Cell cycle arrest, apoptosis induction and inhibition of nuclear factor kappa B activation in anti-proliferative activity of benzyl isothiocyanate against human pancreatic cancer cells. *Carcinogenesis* 2004; **25**: 1701–1709.
16. Aichberger KJ, Mayerhofer M, Krauth MT, Skvara H, Florian S, Sonneck K *et al*. Identification of mcl-1 as a BCR/ABL-dependent target in chronic myeloid leukemia (CML): evidence for cooperative antileukemic effects of imatinib and mcl-1 antisense oligonucleotides. *Blood* 2005; **105**: 3303–3311.
17. Kaufmann SH, Karp JE, Svingen PA, Krajewski S, Burke PJ, Gore SD *et al*. Elevated expression of the apoptotic regulator Mcl-1 at the time of leukemic relapse. *Blood* 1998; **91**: 991–1000.
18. Hussain SR, Cheney CM, Johnson AJ, Lin TS, Grever MR, Caligiuri MA *et al*. Mcl-1 is a relevant therapeutic target in acute and chronic lymphoid malignancies: down-regulation enhances rituximab-mediated apoptosis and complement-dependent cytotoxicity. *Clin Cancer Res* 2007; **13**: 2144–2150.
19. Zhou P, Qian L, Bieszczyk CK, Noelle R, Binder M, Levy NB *et al*. Mcl-1 in transgenic mice promotes survival in a spectrum of hematopoietic cell types and immortalization in the myeloid lineage. *Blood* 1998; **92**: 3226–3239.
20. Moulding DA, Giles RV, Spiller DG, White MR, Tidd DM, Edwards SW. Apoptosis is rapidly triggered by antisense depletion of MCL-1 in differentiating U937 cells. *Blood* 2000; **96**: 1756–1763.
21. Opferman JT, Iwasaki H, Ong CC, Suh H, Mizuno S, Akashi K *et al*. Obligate role of anti-apoptotic MCL-1 in the survival of hematopoietic stem cells. *Science* 2005; **307**: 1101–1104.
22. Opferman JT, Letai A, Beard C, Sorcinelli MD, Ong CC, Korsmeyer SJ. Development and maintenance of B and T lymphocytes requires antiapoptotic MCL-1. *Nature* 2003; **426**: 671–676.
23. Song L, Coppola D, Livingston S, Cress D, Haura EB. Mcl-1 regulates survival and sensitivity to diverse apoptotic stimuli in human non-small cell lung cancer cells. *Cancer Biol Ther* 2005; **4**: 267–276.
24. Nijhawan D, Fang M, Traer E, Zhong Q, Gao W, Du F *et al*. Elimination of Mcl-1 is required for the initiation of apoptosis following ultraviolet irradiation. *Genes Dev* 2003; **17**: 1475–1486.
25. Rahmani M, Davis EM, Bauer C, Dent P, Grant S. Apoptosis induced by the kinase inhibitor BAY 43-9006 in human leukemia cells involves down-regulation of Mcl-1 through inhibition of translation. *J Biol Chem* 2005; **280**: 35217–35227.
26. Maurer U, Charvet C, Wagman AS, Dejaridin E, Green DR. Glycogen synthase kinase-3 regulates mitochondrial outer membrane permeabilization and apoptosis by destabilization of MCL-1. *Mol Cell* 2006; **21**: 749–760.
27. Gao N, Kramer L, Rahmani M, Dent P, Grant S. The three-substituted indolinone cyclin-dependent kinase 2 inhibitor 3-[1-(3*H*-imidazol-4-yl)-meth-(*Z*)-ylidene]-5-methoxy-1,3-dihydro-indol-2-one (SU9516) kills human leukemia cells via down-regulation of Mcl-1 through a transcriptional mechanism. *Mol Pharmacol* 2006; **70**: 645–655.
28. Chen R, Keating MJ, Gandhi V, Plunkett W. Transcription inhibition by flavopiridol: mechanism of chronic lymphocytic leukemia cell death. *Blood* 2005; **106**: 2513–2519.
29. MacCallum DE, Melville J, Frame S, Watt K, Anderson S, Gianella-Borradori A *et al*. Seliciclib (CYC202, *R*-Roscovitine) induces cell death in multiple myeloma cells by inhibition of RNA polymerase II-dependent transcription and down-regulation of Mcl-1. *Cancer Res* 2005; **65**: 5399–5407.
30. Zhong Q, Gao W, Du F, Wang X. Mule/ARF-BP1, a BH3-only E3 ubiquitin ligase, catalyzes the polyubiquitination of Mcl-1 and regulates apoptosis. *Cell* 2005; **121**: 1085–1095.
31. Weng C, Li Y, Xu D, Shi Y, Tang H. Specific cleavage of Mcl-1 by caspase-3 in tumor necrosis factor-related apoptosis-inducing ligand (TRAIL)-induced apoptosis in Jurkat leukemia T cells. *J Biol Chem* 2005; **280**: 10491–10500.
32. Prevot D, Darlix JL, Ohlmann T. Conducting the initiation of protein synthesis: the role of eIF4G. *Biol Cell* 2003; **95**: 141–156.
33. Holcik M, Sonenberg N. Translational control in stress and apoptosis. *Nat Rev Mol Cell Biol* 2005; **6**: 318–327.
34. Vary TC, Lynch CJ. Nutrient signaling components controlling protein synthesis in striated muscle. *J Nutr* 2007; **137**: 1835–1843.
35. Harris TE, Chi A, Shabanowitz J, Hunt DF, Rhoads RE, Lawrence Jr JC. mTOR-dependent stimulation of the association of eIF4G and eIF3 by insulin. *EMBO J* 2006; **25**: 1659–1668.
36. Quevedo C, Salinas M, Alcazar A. Regulation of cap-dependent translation by insulin-like growth factor-1 in neuronal cells. *Biochem Biophys Res Commun* 2002; **291**: 560–566.
37. Zhang B, Gojo I, Fenton RG. Myeloid cell factor-1 is a critical survival factor for multiple myeloma. *Blood* 2002; **99**: 1885–1893.
38. Gao N, Budhraja A, Cheng S, Yao H, Zhang Z, Shi X. Induction of apoptosis in human leukemia cells by grape seed extract occurs via activation of c-Jun NH2-terminal kinase. *Clin Cancer Res* 2009; **15**: 140–149.



Cell Death and Disease is an open-access journal published by Nature Publishing Group. This work is licensed under the Creative Commons Attribution-NonCommercial-No Derivative Works 3.0 Unported License. To view a copy of this license, visit <http://creativecommons.org/licenses/by-nc-nd/3.0/>